Superparamagnetic nanoparticle-supported palladium: a highly stable magnetically recoverable and reusable catalyst for hydrogenation reactions

Liane M. Rossi,*[a] Fernanda P. Silva,[a] Lucas L. R. Vono,[a] Pedro K. Kiyohara,[b] Evandro L. Duarte,[b] Rosangela Itri,[b] Richard Landers[c] and Giovanna Machado[d]

Received 7th September 2006, Accepted 2nd January 2007
First published as an Advance Article on the web 24th January 2007
DOI: 10.1039/b612980c

Here we present a magnetically recoverable palladium catalyst prepared by immobilization of palladium over silica-coated magnetite nanoparticles. The catalyst reduced by molecular hydrogen contains palladium nanoparticles well distributed and stabilized in the magnetizable support surfaces and converts cyclohexene to cyclohexane under mild reaction conditions (75 °C and 6 atm) with TOF of 11 500 h^{-1}. The catalyst was easily recovered with a permanent magnet in the reactor wall and reused for up to 20 recycles of 2500 TON each without any significant loss in catalytic activity, demonstrating an efficient recycling process for hydrogenation reactions.

Introduction

Superparamagnetic nanoparticles are now emerging as new supporting materials for catalysts immobilization with increased catalyst to products separation capabilities.[1] Nanometric iron oxides respond to an external magnetic field but do not remain magnetized when the magnetic field is removed. These properties permit superparamagnetic materials to be concentrated from the solution with a magnet and dispersed immediately after removing the magnetic field. The absence of remanence prevents particle–particle attraction and particle aggregation, which would dramatically decrease the surface area of a solid support. Magnetic separation is very promising to greatly improve separability and recycling of homogeneous and nanocluster catalysts. In this recycling process, the catalyst can be magnetically recovered inside the reactor vessel while draining the liquid products. It can be considered a greener technology that avoids the consequences of filtration steps such as catalyst mass loss, catalyst oxidation, use of additional solvents and the subsequent generation of organic residues.

Magnetic separation has been extensively used in biomedical applications such as drug targeting, cell sorting and isolation and separation of biochemical products.[2] The biomedical applicability of magnetic particles is greatly improved by coating their surfaces to protect the magnetic core and increase surface reactivity. It is worth mentioning the results of Philipse *et al.*[3] and Xia *et al.*[4] on the preparation of silica coated magnetic nanoparticles. Silica contains reactive silanol groups that can be easily functionalized by organosilanes yielding modified surfaces with a variety of functional groups, such as amino and thiol.[5] Those functional groups can also work perfectly as coordinating sites for metals as well as starting materials for the engineering of chelant ligands on silica surfaces. Thiol-modified mesoporous silica, for instance, has been shown as a remarkable scavenger for palladium.[6,7] The palladium loaded solid obtained by Crudden *et al.*[7] was also used as a heterogeneous and reusable catalyst for coupling reactions with no leaching of palladium (<3 ppb Pd in the filtrates). Immobilization of palladium on solid supports is a strategy to decrease the accumulation of palladium in the final products, especially important in the synthesis of pharmaceuticals, but leaching of palladium can occur. In some cases, it has been demonstrated that heterogeneous catalysts are merely reservoirs for highly active soluble forms of palladium.[8] In an attempt to prepare a palladium-based magnetically separable catalyst we first coated the surfaces of superparamagnetic nanoparticles with silica and then modified their surfaces with thiol for the immobilization of palladium. The catalyst, reduced by molecular hydrogen, contains palladium nanoparticles well distributed and stabilized in the magnetizable support surfaces. The catalytic performance and recycling of the magnetizable palladium catalyst in hydrogenation reactions in solventless conditions were investigated.

Results and discussion

Silica-coated magnetic particles were prepared following the procedure described by Philipse *et al.*[3] that consists of pre-coating magnetic particles surfaces with soluble silicate, and subsequent growth of a silica layer by condensation of tetraethylorthosilicate. The pre-coating step was necessary to improve the solubility of the magnetic particles in the alcohol mixture that is used for the silica layer growth. Without this step, precipitation and agglomeration of the magnetic nanoparticles take place immediately after addition of ethanol or isopropanol. The magnetic cores were prepared by co-precipitation of Fe^{2+}/Fe^{3+} ions under alkaline conditions followed by stabilization with tetraethylammonium hydroxide.[3] TEM images of the pre-coated magnetic particles and the silica-coated magnetic spheres are shown in Fig. 1 and 2. Analysis of the micrograph in Fig. 1a indicates that these

[a]*Institute of Chemistry, University of São Paulo, USP, São Paulo, 05508-000, SP, Brazil and CEPEMA-USP, Cubatão, SP, Brazil. E-mail: lrossi@iq.usp.br1; Fax: +55 11 38155579; Tel: +55 11 30912181*
[b]*Institute of Physics, USP, São Paulo, SP, 05508-090, Brazil*
[c]*Institute of Physics, UNICAMP, Campinas, SP, 13083-970, Brazil*
[d]*Institute of Chemistry, UFRGS, Porto Alegre, RS, 91501-970, Brazil*

This journal is © The Royal Society of Chemistry 2007

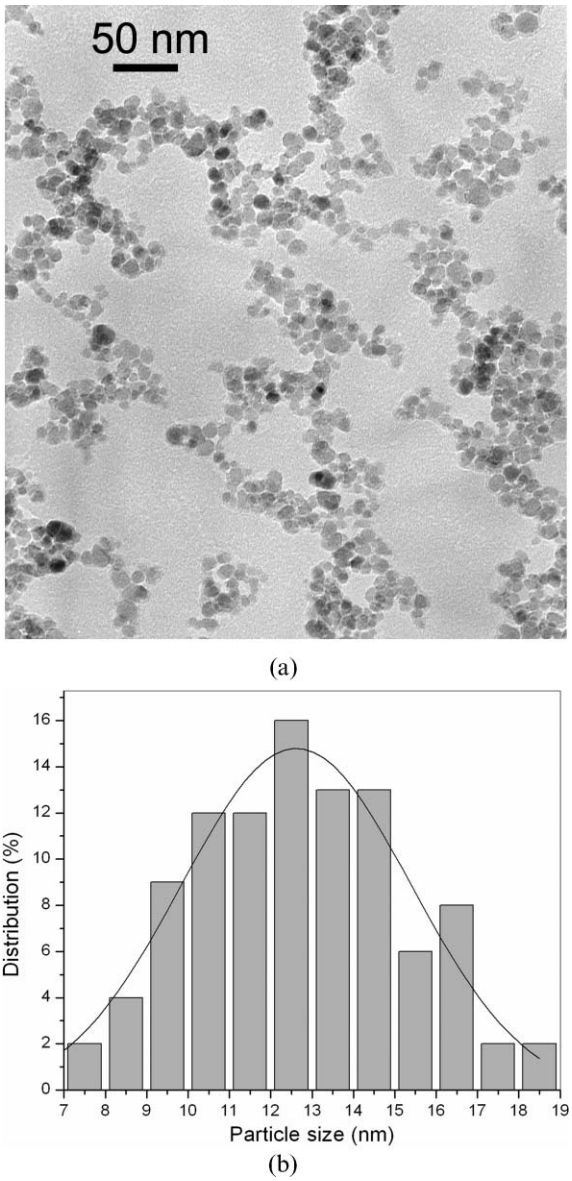

Fig. 1 (a) Transmission electron microscopy (TEM) of the pre-coated magnetite nanoparticles and (b) histogram showing particle size distribution.

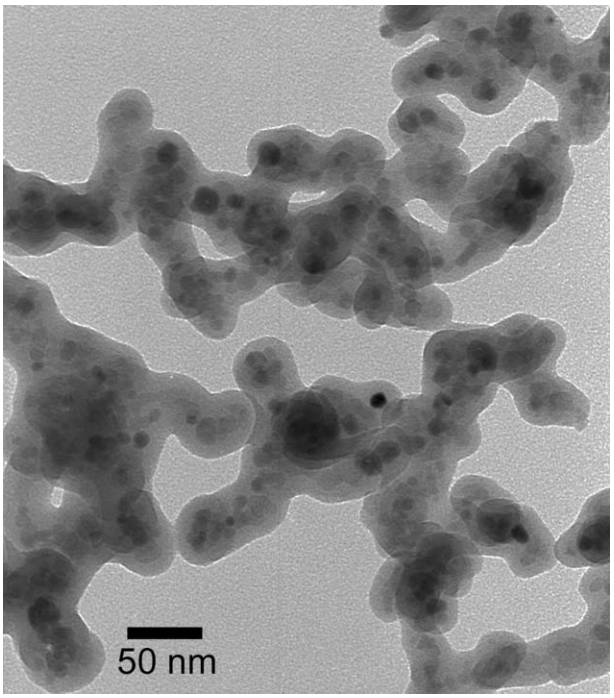

Fig. 2 TEM of silica-coated magnetic spheres.

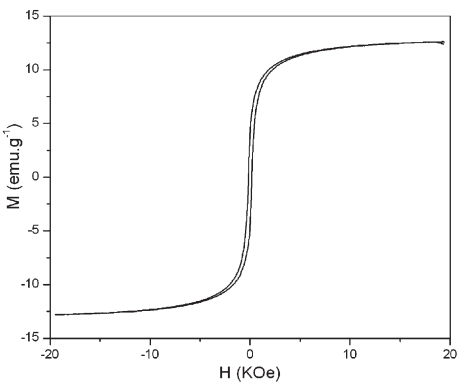

Fig. 3 Magnetization curve of silica-coated magnetic particles at 300 K.

nanoparticles display an irregular shape, but evaluating their characteristic diameter results in a mono modal distribution. The histogram of Fig. 1b shows that particle size distributions can be reasonably well fitted by a Gaussian curve. The average diameter of the nanoparticles after pre-coating with silicate, determined by measuring the diameter of 600 randomly selected particles in enlarged TEM images, was 12 ± 3 nm.

After a 10 nm silica layer growth, the particles size increased to approximately 30 to 40 nm diameter size (Fig. 2). Although most of the particles appear spherical in shape, some aggregation can be seen and we were not able to precisely determine particles size.

Magnetization curves revealed the superparamagnetic behavior of the silica coated-magnetic nanoparticles with a saturation magnetization of 12.6 emu g^{-1} (Fig. 3). This value is smaller than that of bulk magnetite (92 emu.g^{-1}), which is consistent with the presence of a diamagnetic component. The decrease of the saturation magnetization suggests the presence of 30% of silica in the material.[9] Even with this reduction in the saturation magnetization the solid can still be efficiently separated from solution with a small neodymium permanent magnet ($\sim$4400 G).

The silica-coated magnetic particles had their surfaces modified with thiol groups through hydrolysis and condensation with 3-mercaptopropyltrimethoxysilane (MPTMS), performed in dry toluene under nitrogen to minimize side-reaction. A thermal curing of the silanized solids was included to guarantee a stable, cross-linked and condensed silane layer.[5] The mercaptopropyl-modified silica coated magnetic particles were submitted to an aqueous solution of $[PdCl_4]^{2-}$ (1.0 mg mL^{-1}). The isolated solid contains 1.21 wt% of palladium as determined by ICP-AES. The catalytic activity of the magnetizable palladium catalyst was investigated in

 This journal is © The Royal Society of Chemistry 2007

Table 1 Hydrogenation of cyclohexene to cyclohexane by Pd magnetically recoverable catalyst

Entry	*P*/atm	*T*/°C	Time/min	Conv. (%)[a]	TON[b]	TOF[c]/h^{-1}
1	6	75	13	>99	2500	11 538
2	4	75	18	>99	2500	8333
3	2	75	51	>99	2500	2941
4	1	75	152	>99	2500	987
5	6	25	22	96	2400	6545
6	1	25	120	56	1400	700
7	6	75	510	>99	50 000	5882
8[d]	6	75	600	>99	50 000	5000
9[e]	10	75	240	3	27	7

[a] Measured by GC. [b] Catalytic turnover number: mol of substrate transformed per mol of catalyst. [c] Catalytic turnover frequency: mol of substrate transformed per mol of catalyst per hour. [d] Catalyst reused after experiment described in entry 7. [e] Reaction performed without Pd: magnetic particles/substrate ratio = 1/1000.

hydrogenation reactions of olefins to the corresponding alkanes in solventless conditions. The reactor loaded with the catalyst and the olefin was submitted to the desired hydrogen pressure and temperature. The reaction is monitored by the consumption of hydrogen in a reservoir connected to the main reactor maintained at constant pressure. Curves of hydrogen pressure *versus* time were obtained for each experiment. At the desired time, the reactor was cooled down, the remaining hydrogen relieved and the catalyst recovered magnetically by placing a magnet in the reactor wall. The organic phase was easily separated and analyzed by gas chromatography. Table 1 summarizes the results.

The hydrogenation of cyclohexene at P_{H_2} = 6 atm and T = 75 °C showed a very high turnover frequency of 11 500 h^{-1} (Table 1, entry 1). At a hydrogen pressure of 1 atm, the reaction became ten times slower at 75 °C (Table 1, entry 4) and did not go to completion after two hours at 25 °C (Table 1, entry 6). Similar experiments performed with non-supported $PdCl_2$ showed deposition of a metallic film and catalyst deactivation. The performance of commercially available Pd/C catalyst under the conditions used in this study is comparable to our results (TOF = 18 750 h^{-1}), but with the difficulty of separating the product. The catalytic parameters shown in Table 1 were calculated based on the total amount of palladium in the catalyst without taking into account the true number of active metal sites on nanoparticles surfaces, consequently those values may be underestimated.[10] The values shown in Table 1 are higher than those reported for hydrogenation of cyclohexene by palladium[11] and other metal nanoparticles[12] stabilized in solid or liquid supports.

Further experiments were performed to verify the catalyst stability and recyclability. After a first run with complete conversion of 28 mmol of olefin (11.2 μmol palladium, 75 °C and 6 atm H_2), the magnetically recovered catalyst was reused in twenty successive runs of 2500 TON each (total turnover of 50 000 in 9 h), by addition of new portions of cyclohexene. The catalyst showed no significant loss of activity at the end of the 20th run (Fig. 4). Variations on the reaction rates in the series of experiments were observed, but the rate of the first and the 20th batch were the same (5000 h^{-1}), which means that the active metal sites were maintained. Moreover, the minimum activity (lower TOF values) did not change significantly, but peaks of increased activity were observed at recharges 6, 12, 13, 15 and 18. The organic products were collected and the Pd content was <0.01 ppm (ICP-AES analysis). In order to better estimate the catalyst lifetime, a new experiment was performed with an olefin/Pd ratio of 50 000 (Table 1 entry 7) and the catalyst was still active for a second run (Table 1, entry 8) corresponding to a total turnover (TTO) of 100 000.

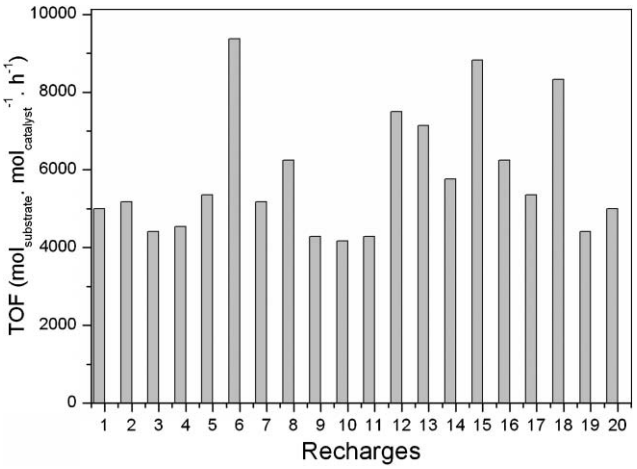

Fig. 4 Catalyst recycling in the hydrogenation of cyclohexene at 2500 mol substrate per mol catalyst each run, 75 °C and 6 atm H_2.

In order to obtain evidence that reduction of the Pd(II) bonded to mercaptopropyl modified magnetic solid occurred when submitted to hydrogenation conditions, we carried out TEM (Fig. 5), X-ray diffraction (XRD) (Fig. 6) and X-ray photoelectron spectroscopy (XPS) (Fig. 7) analysis of the spent catalyst. The results shown in Fig. 5 and Fig. 6 are consistent with the formation of $[Pd(0)]_n$ nanoparticles on silica surfaces of the catalyst submitted to hydrogenation reactions.

The stabilization of metal nanoparticles on the magnetic support surface can explain the high reusability of our catalyst without losing activity. It is well established that high energy surface metal nanoparticles aggregate into larger particles or bulk materials in the absence of stabilizing agents or supports, resulting in decreased surface areas, loss of reactive sites and consequently deactivation of the catalyst by agglomeration.[13]

The TEM image of the spent catalyst (Fig. 5a) clearly shows the silica shell decorated with very small particles, attributed to palladium species since they were absent in the TEM image of the silica-coated magnetic particles shown in Fig. 2. Analysis of TEM enlarged micrographs, by measuring the diameter of 300 randomly selected particles, resulted in the particle size distribution histogram shown in Fig. 5b. The size distribution was found to be well described by a Gaussian distribution function from which we obtained an average particle diameter of 3.0 ± 0.5 nm. The high resolution TEM (HRTEM) image (Fig. 5c) allowed us, by means of Gatan software, to obtain the Fourier transform from which lattice spacings of 2.16 and 2.02 Å were (experimental error <5%). These lattice spacings, corresponding to the interplanar distance (1 1 1) and (2 0 0) of the Pd(0), are depicted by the arrows in Fig. 5c.

The XRD pattern of the spent catalyst confirms the presence of crystalline Pd(0) by the appearance of the most representative Bragg reflections of Pd(0) metal as indicated in the Fig. 6(b). The mean diameter could be estimated from the

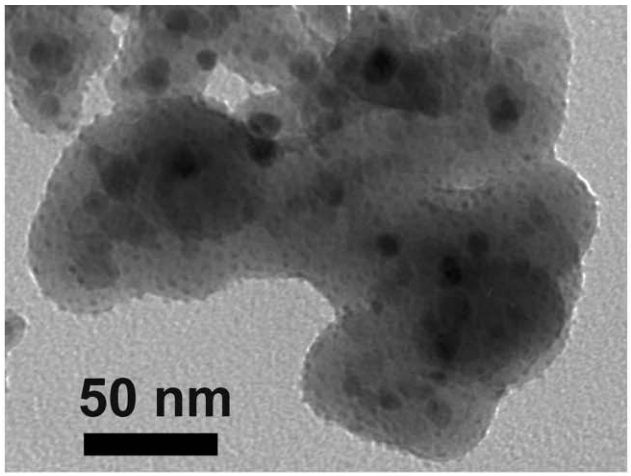

(a)

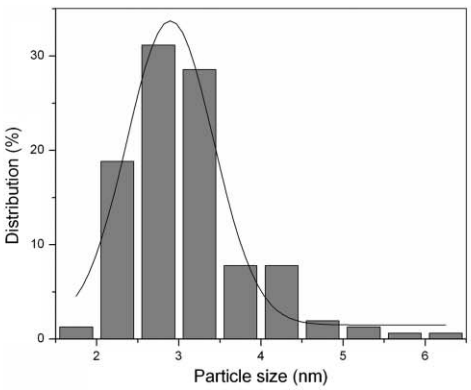

(b)

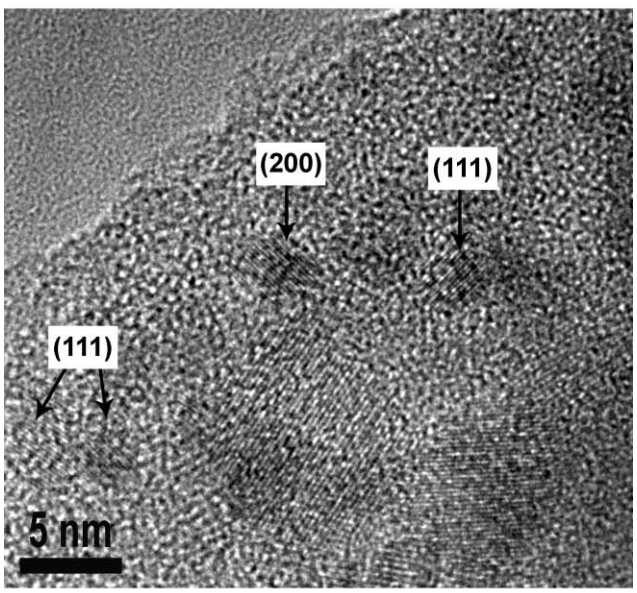

(c)

Fig. 5 (a) TEM micrographs, (b) histograms showing the particle size distribution of Pd(0), and (c) HRTEM image of the spent catalyst with the interplanar distance indicated by arrows.

XRD diffraction pattern by means of the Debye–Scherrer equation calculated from full width at half-maximum (fwhm) of the (111), (200), (220), (311), and (222) planes obtained from Rietveld's refinements. The most representative reflections of

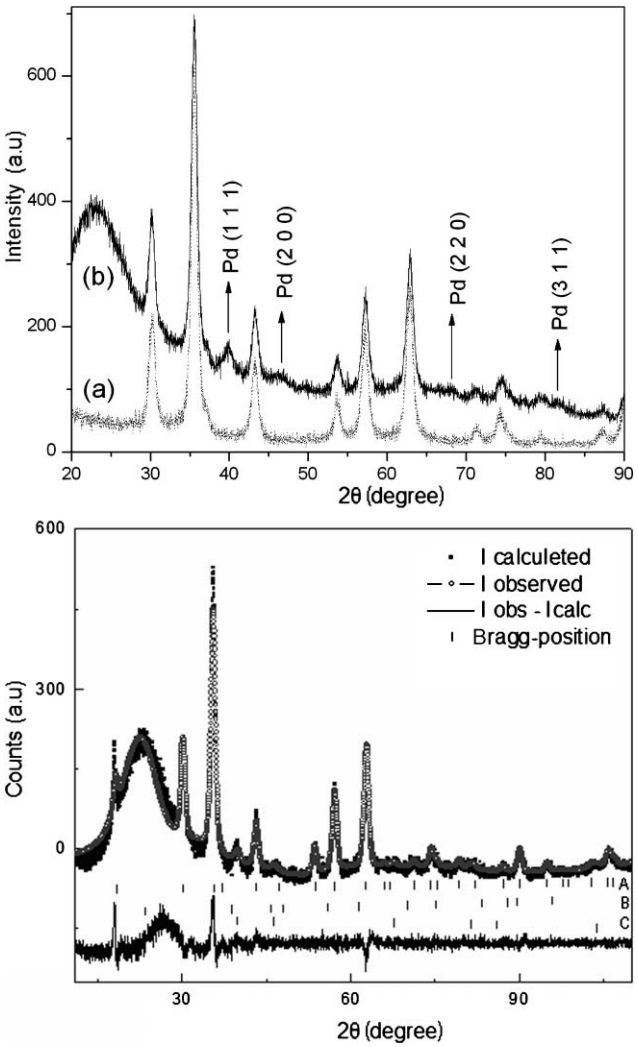

Fig. 6 X-ray diffraction pattern of (a) the magnetic core—Fe_3O_4 nanoparticles and (b) the spent catalyst (top) and Rietveld's refinement (bottom). (A = Bragg peak position Fe_3O_4; B = Bragg peak position SiO_2; C = Bragg peak position Pd (0)).

Pd(0) and Fe_3O_4 were indexed as face-centered cubic (fcc) with unit cell parameter a = 3.9142 Å and a = 8.3668 Å, respectively. The simulations of Bragg reflections and Rietveld's refinement were performed with a pseudo-Voigt function using

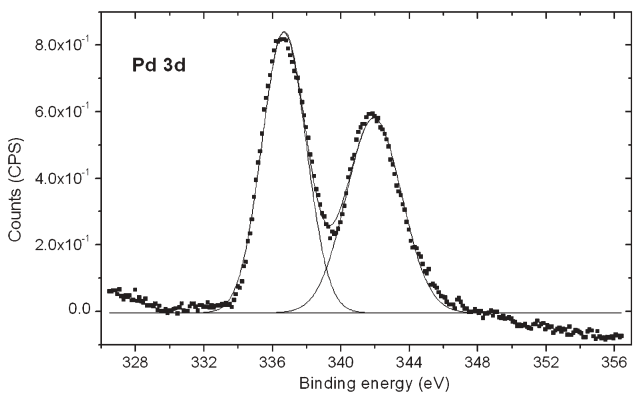

Fig. 7 XPS spectrum of the spent catalyst.

This journal is © The Royal Society of Chemistry 2007

the FULLPROF code.[14] It is important to point out that the use of fwhm of a peak to estimate the size of crystalline grain by means of the Scherrer equation has serious limitations, since it does not take into account the existence of a distribution of sizes and the presence of defects in the crystalline lattice. Therefore, the calculation of the average diameter of the grains from fwhm of the peak can overestimate the real value, since the larger grains give a strong contribution to the intensity, while the smaller grains just enlarge the base of the peak. Moreover, the presence of defects in a significant amount causes an additional enlargement of the diffraction line. Considering this enlargement, the obtained size can be smaller than the real size of the grains. These problems can be minimized by the use of Rietveld's refinement method. Indeed, these discrepancies are confirmed by the values found for the average diameter of the nanoparticles without the structural refinement (8.5 $\pm$ 3 nm and 6.5 nm), which significantly differ from those found by means of Rietveld's refinement (11.5 $\pm$ 3 nm and 4.5 nm) for the nanoparticles Fe_3O_4 and Pd(0), respectively. These latter values are much closer to those determined by TEM. Fig. 6 shows the X-ray diffraction pattern of the magnetic core—Fe_3O_4 nanoparticles, the spent catalyst (top) and Rietveld's refinement of this material (bottom).

Further analysis of the spent catalyst using XPS showed the palladium 3d doublet at 336.7 eV for $3d_{5/2}$ and 341.9 eV for $3d_{3/2}$ (Fig. 7). According to the literature,[15] the Pd $3d_{5/2}$ peak binding energy for Pd(0) is 335.1 eV. However, we found the Pd $3d_{5/2}$ peak shifted to higher values, suggesting that the catalyst has electron-deficient palladium species on the surface. These oxidized forms of Pd might be palladium chloride or palladium oxide, which show Pd $3d_{5/2}$ peak binding energies at 337.5 or 336.9 eV, respectively.[15] Considering the peak position, TEM and XRD results, the Pd(II) component found in our system can be attributed to PdO, probably resulting from surface reoxidation of high surface area palladium nanoparticles during workup procedures. Analysis of peak binding energies also confirms the absence of the metal precursor, palladium chloride, in the spent catalyst. Using the same sample portion, a new XRD analysis was performed and, again, the most representative Bragg reflections of Pd(0) metal were observed in the XRD pattern, whereas the expected Bragg reflections of crystalline PdO were not detected. These results are consistent with the presence of an amorphous layer of PdO over the palladium nanoparticles only detected by XPS and not detected by XRD.

Conclusions

In summary, we have prepared a highly stable magnetically recoverable catalyst formed by very small palladium nanoparticles well distributed and stabilized in the magnetizable support surfaces. A good agreement was found between TEM and XRD methods for determining the mean relative diameters of the nanoparticles. The values obtained were 3.0 and 4.5 nm from TEM and XRD, respectively. The catalyst showed excellent catalytic activity for hydrogenation of cyclohexene without catalyst leaching or deactivation after 20 cycles or 100 000 turnovers. After each reaction, the catalyst could be easily separated magnetically from the reaction products minimizing the generation of organic residues and avoiding the use of additional solvents and environmentally non-friendly procedures.

Experimental

Materials and instrumentation

Iron(II) chloride hydrate, iron(III) chloride hydrate, ammonium hydroxide, 3-mercaptopropyltriethoxysilane, tetraethylammonium hydroxide, tetraethoxysilane and cyclohexene were purchased from Aldrich and Fluka and used without further purification.

GC analysis. Gas chromatography analyses were performed on a Shimadzu GC 17A, equipped with a 30 metre capillary column with a dimethylpolysiloxane stationary phase, using the following parameters: initial temperature: 40 °C, initial time: 5 min, ramp: 10 °C min^{-1}, final temperature: 250 °C, final time: 5 min, injector and detector temperature: 250 °C, injection volume: 2 μL.

TEM analysis. The morphology of the obtained nanoparticles was obtained on a Philips CM 200 operating at an accelerating voltage of 200 kV. The samples for TEM were prepared by dispersion of the nanoparticles in aqueous solution at room temperature and then collected on a carbon-coated copper grid. The histograms of the nanoparticles size distribution, assuming spherical shape, were obtained from the measurement of about 600 particles and were reproduced in different regions of the Cu grid, found in an arbitrarily chosen area of enlarged micrographs. The high resolution electron microscopy work was performed with a JEM-3010 ARP microscope.

XRD analysis. The phase structures of nanoparticles were characterized by XRD. For the XRD analysis, the nanoparticles were isolated as a fine powder and placed in the sample holder. The XRD experiments were carried out on a Rigaku-Denki powder diffractometer equipped with a curved graphite crystal using Cu Kα radiation λ = 1.5418 Å. The diffraction data were collected at room temperature in a Bragg–Brentano θ–2θ geometry with scan range between 10° to 100°. The diffractograms were obtained with a constant step, $\Delta 2\theta$ = 0.02°. The indexation of Bragg reflections was obtained by a pseudo-Voigt profile fitting using the FULLPROF code.[14]

Magnetic measurements. A VSM was used to obtain the magnetization *versus* magnetic field loop at room temperature up to H = 20 kOe. The apparatus was calibrated with a Ni pattern. The magnetization measurements were carried out on a known quantity of powder samples, slightly pressed and conditioned in cylindrical holders of Lucite.

XPS analysis. The X-ray photoelectron spectra were obtained with a VSW HA-100 spherical analyzer using an aluminum anode (AlKα line, hv = 1486.6 eV) X-ray source. The high-resolution spectra were measured with constant

analyzer pass energies of 44 eV, which produce a full width at half-maximum (fwhm) line width of 1.7 eV for the Au($4f_{7/2}$) line. The powdered samples were pressed into pellets and fixed to a stainless steel sample holder with double-faced tape and analyzed without further preparation. To correct for charging effects the spectra were shifted so that the C1s binding energy was 284.6 eV. Curve fitting was performed using Gaussian line shapes, and Shirley type background was subtracted from the data.

Synthesis of magnetic particles. Fe_3O_4 nanoparticles were prepared by the co-precipitation method: 10 mL of an aqueous solution of $FeCl_3$ (1 mol L^{-1}) were mixed with 2.5 mL of $FeCl_2$ (2 mol L^{-1}) dissolved in HCl 2 mol L^{-1}. Both solutions were freshly prepared with deoxygenated water before use. Immediately after being mixed under nitrogen, the solution containing the iron chlorides was added to 125 mL of ammonium hydroxide solution (0.7 mol L^{-1}, deoxygenated water) under vigorous mechanical stirring (10 000 rpm, Ultra-Turrax T18 Homogenizer, IKA Works), under nitrogen atmosphere. After 30 minutes, the black precipitate formed was separated magnetically and redispersed in a new portion of water (3 × 250 mL). The obtained precipitate was dispersed in 125 mL of water and stabilized after addition of 15 mL of tetraethylammonium hydroxide.

Synthesis of magnetic silica spheres. Silica-coated magnetic particles were prepared following the procedure described by Philipse *et al.*[3] A 16 mL of a 0.58 wt% silicate solution (the silicate solution was previously passed through an acid exchange resin column and the pH adjusted to 9.5 using a small portion of the original silicate solution) was mixed with 85 mL of ferrofluid stabilized with tetraethylammonium hydroxide (1.4 g L^{-1}). After the mixture, the solution attained pH 12 and was adjusted to pH 10 with 0.5 mol L^{-1} HCl. The solution was stirred for 2 h and submitted to dialysis against an aqueous solution of tetraethylammonium hydroxide with pH adjusted to 10 for 2 days. Further silica growth on the obtained particles was performed according to the Stöber method. To a solution containing 944 mL of ethanol, 34 mL of NH_4OH and 9.1 mL of the obtained particles was added 0.8 mL of TEOS. The solution was allowed to stand for 24 h under stirring. The product was isolated by centrifugation (6000 rpm, 20 min) and washed with ethanol (3 × 50 mL) and water (2 × 50 mL) and dried in oven at 100 °C overnight.

Synthesis of mercaptopropyl-modified magnetic silica spheres. The reaction was performed under nitrogen using Schlenk techniques and dry solvent. To a dispersion containing 200 mg of magnetic silica spheres in toluene (15 mL) was added 0.15 mL of 3-mercaptopropyltriethoxysilane (MPTS). The solution was stirred for 2 hours. The resulting precipitate was centrifuged (6000 rpm, 10 min) and washed with toluene and acetone and dried in oven at 100 °C for 20 h. Elemental analysis: 2.04% C, 0.85% H.

Preparation of palladium catalyst. To 50 mg of thiol-modified magnetic silica spheres was added 5 mL of a palladium chloride solution (1 mg mL^{-1}) ($PdCl_2$ was dissolved in water by addition of NaCl and heating). The resulting solid was separated magnetically, washed with water and acetone and isolated as a powder. Palladium contents (analyzed by ICP-AES): 1.21 wt%

Hydrogenation experiments. The catalytic reactions were carried out in a Fischer–Porter reactor connected to an H_2 reservoir. In a typical experiment, catalyst (50 mg, 5.6 μmol Pd) and 1.16 g of cyclohexene (14 mmol) are added to the reactor under inert atmosphere. The reactor is connected to a hydrogen gas reservior and the reaction is initiated by the gas admission at constant pressure. The reaction is monitored by the fall in hydrogen pressure in the H_2 reservoir as a function of time. H_2 uptake was measured in 10 sec intervals with a pressure transmitter interfaced *via* a Novus Field Logger converter to a computer. The pressure *versus* time data are collected by the FieldChart Novus Software, stored as a data file and exported to MicroCal Origin 7.0 for hydrogenation rates calculations. The catalyst is recovered magnetically by placing a magnet in the reactor wall and the products are collected and analyzed by GC and GC-MS. The isolated catalyst can be reused by addition of new portions of substrate.

Acknowledgements

We are grateful to FAPESP, CNPq and TWAS for financial support. We also thank the Laboratory of Magnetism of IF-USP for VSM measurements, and the Laboratory of Electron Microscopy of LNLS, Campinas, SP for HRTEM images.

References

1 T.-J. Yoon, W. Lee, Y.-S. Oh and J. K. Lee, *New J. Chem.*, 2003, **27**, 227; P. D. Stevens, G. Li, J. Fan, M. Yen and Y. Gao, *Chem. Commun.*, 2005, 4435; P. D. Stevens, J. Fan, H. M. R. Gardimalla, M. Yen and Y. Gao, *Org. Lett.*, 2005, **7**, 2085; A. Hu, G. T. Yee and W. Lin, *J. Am. Chem. Soc.*, 2005, **127**, 12486; M. Kotani, T. Koike, K. Yamaguchi and N. Mizuno, *Green Chem.*, 2006, **8**, 735.

2 Q.A. Pankhurst, J. Connolly, S. K. Jones and J. Dobson, *J. Phys. D: Appl. Phys.*, 2003, **36**, R167 and references therein; Z. M. Saiyed, S. D. Telang and C. N. Ramchand, *Biomagn. Res. Technol.*, 2003, **1**, 2; S. K. Sahoo and V. Labhasetwar, *Drug Discovery Today*, 2003, **8**, 1112.

3 A. P. Philipse, M. P. B. van Bruggen and C. Pathmamanoharan, *Langmuir*, 1994, **10**, 92.

4 Y. Lu, Y. Yin, B. T. Mayers and Y. Xia, *Nano Lett.*, 2002, **2**, 183.

5 I. Haller, *J. Am. Chem. Soc.*, 1978, **100**, 8050; C. M. Halliwell and A. E. G. Cass, *Anal. Chem.*, 2001, **73**, 2476; K. C. Vrancken, L. D. Coster, P. V. D. Voort, P. J. Grobet and E. F. Vansant, *J. Colloid Interface Sci.*, 1995, **170**, 71.

6 T. Kang, Y. Park, J. C. Park, Y. S. Cho and J. Yi, *Stud. Surf. Sci. Catal.*, 2003, **146**, 527; T. Kang, Y. Park and J. Yi, *Ind. Eng. Chem. Res.*, 2004, **43**, 1478.

7 C. M. Crudden, M. Sateesh and R. Lewis, *J. Am. Chem. Soc.*, 2005, **127**, 10045.

8 K. Yu, W. Sommer, J. M. Richardson, M. Weck and C. W. Jones, *Adv. Synth. Catal.*, 2005, **347**, 161; A. Biffis, M. Zecca and M. Basato, *Eur. J. Inorg. Chem.*, 2001, 1131.

9 P. S. Haddad, E. L. Duarte, M. S. Baptista, G. F. Goya, C. A. P. Leite and R. Itri, *Prog. Colloid Polym. Sci.*, 2004, **128**, 232.

10 L. M. Rossi, G. Machado, P. F. P. Fichtner, S. R. Teixeira and J. Dupont, *Catal. Lett.*, 2004, **92**, 149; J. A. Widegren and R. G. Finke, *J. Mol. Catal. A: Chem.*, 2003, **198**, 317.

11 J. Huang, T. Jiang, B. Han, H. Gao, Y. Chang, G. Zhao and W. Wu, *Chem. Commun.*, 2003, 1654; J. Huang, T. Jiang, H. Gao, B. Han, Z. Liu, W. Wu, Y. Chang and G. Zhao, *Angew. Chem.,*

 This journal is © The Royal Society of Chemistry 2007

Int. Ed., 2004, **43**, 1397; M. Ooe, M. Murata, T. Mizugaki, K. Ebitani and K. Kaneda, *Nano Lett.*, 2002, **2**, 999.
12 See for example: L. M. Rossi, J. Dupont, G. Machado, P. F. P. Fichtner, C. Radtke, I. J. R. Baumvol and S. R. Teixeira, *J. Braz. Chem. Soc.*, 2004, **15**, 904; J. Dupont, G. S. Fonseca, A. P. Umpierre, P. F. P. Fichtner and S. R. Teixeira, *J. Am. Chem. Soc.*, 2002, **124**, 4228; C. W. Scheeren, G. Machado, J. Dupont, P. F. P. Fichtner and S. R. Texeira, *Inorg. Chem.*, 2003, **42**, 4738; C. W. Scheeren, G. Machado, S. R. Texeira, J. Morais, J. B. Domingos and J. Dupont, *J. Phys. Chem. B*, 2006, **110**, 13011; X. Mu, D. G. Evans and Y. Kou, *Catal. Lett.*, 2004, **97**, 151; J. Schulz, A. Roucoux and H. Patin, *Chem. Commun.*, 1999, 535; A. M. Doyle, S. K. Shaikhutdinov, S. D. Jackson and H.-J. Freund, *Angew. Chem., Int. Ed.*, 2003, **42**, 5240; J. D. Aiken, III and R. G. Finke, *J. Am. Chem. Soc.*, 1999, **121**, 8803.
13 G. Schmid, *Chem. Rev.*, 1992, **92**, 1709.
14 J. R. Carbajal, *Short Reference Guide of The Program Fullprof, version 2005*, http://valmap.dfis.ull.es/fullprof/php/downloads.php.
15 C. D. Wagner, W. M. Riggs, L. E. Davis and J. F. Moulder, in *Handbook of X-ray Photoelectron Spectroscopy*, ed. G. E. Muilenberg, Perkin–Elmer Corporation, Eden Prairie, MN, USA, 1978.